

The effect of jet angle and velocity ratio on turbine blade film cooling

A. K. Al Taie¹ & M. S. Kassim²

¹*University of Technology, Baghdad, Iraq*

²*University of Mustansiriya, Baghdad, Iraq*

Abstract

This work is concerned with the thermal effect of the turbine blade by film cooling. The jet flow penetration and flow structure was simulated and solved numerically. This investigation presents a tool to obtain qualitative information about the penetration area and flow structure of the mixing flow at different jet angle configurations. Two models of airfoil (NACA 0021) with hole diameters, $d=0.1$ and 0.2 cm were studied. The simulation was carried out using the commercial code (FLUENT 6.3). Several cases were considered; including three-velocity ratio, $VR=0.3, 0.7, 1, 1.5, 2$ and two jet suction angles, β of 37.5° and 90° , and four different angles of attack, $\alpha=0^{\circ}, 5^{\circ}, 10^{\circ},$ and 15° . The cooling films build up on the blade surface was simulated. The work gives a clear picture of the penetration area for the normal and angled-injection cases. The results at different sections, $x/s=0.5$ and 0.9 for the first and second model provided the optimum holes rows spacing and the low suction angle for maximum film cooling effectiveness.

Keywords: gas turbine, blade cooling, jet flow, numerical simulation, film cooling.

1 Introduction

The blades/vanes in gas turbines require proper cooling mechanisms to protect the material from thermal stresses generated by exposure to hot combustion gases. The problem becomes aggravated by the growing trend of using higher turbine inlet temperature to generate more power. Thus, film cooling is used as a cooling mechanism and it works in the form of row of holes in the span wise directions of the blade, from where cold jet is issued into the hot cross flow. The



mixing process during the penetration of the cold jet into the hot gas creates a three-dimensional flow field. The resulting temperature downstream of the jet, the trajectory and physical path of the jet are critical design parameters [1]. Film cooling flows are characterized by cooling jet injected at an angle from the blade surface into the heated cross flow. The resulting flow field is quite complex, and accurate predictions of the flow and heat transfer have been difficult to obtain, particularly in the near field of the injected jet [2]. Therefore the flow penetration, flow structure, and the thermal effect of cooling jets issuing into an incompressible hot cross flow at an angle over an airfoil which represents the turbine blade surface are the main objects in the present study. In order to provide an assessment of the performance of different models, a film cooling configuration that was geometrically simple, but which incorporated all the essential physics of the film cooling problem was chosen.

Embedding film cooling holes in slots (Bunker [3]), trenches (Waye and Bogard [4]) to simulate thermal barrier coating sprays, and downstream of backward facing steps (Rallabandi *et al.* [5]) have been found to increase film cooling effectiveness in the proximity of the hole. A large semi-cylinder is conventionally used as a good approximation to the stagnation region on a turbine blade. The use of shaped holes to improve film coverage has been studied by (Gao and Han [6]). (Je-Chin Han and Rallabandi [7]) have investigated the PSP method that provides very high resolution contours of film cooling effectiveness, without being subject to the conduction error in high thermal gradient regions near the hole. (Kini *et al.* [8]) have analyzed computationally the coupled conjugate analysis of HP stage turbine blade for effective cooling using innovative cooling passages within the blade. A helicoidally shaped duct has been analyzed corresponding to different diameters and pitch length. It is found from that helicoidally cooling duct with larger diameter and with lower pitch length provides a vastly improved blade cooling in comparison to straight ducted cooling ducts for the HP stage turbine blade.

2 Numerical analysis

In order to develop an applicable comprehensive computational method, some reasonable assumptions have to be made, these are:-

The entering fluid flow is subsonic everywhere, the fluid flow is incompressible.

The fluid flow is steady and fully viscous. The turbulence is isotropic.

The flow within the coolant hole is three-dimensional [2]. A separation at the hole inlet is the cause of a pair of counter-rotating vortices and a region of increased velocity opposite to the separation bubble. The blockage created by the jet as it enters the mainstream creates a local variation in pressure at the hole exit. After leaving the hole, the coolant mixes with the mainstream. An approximation of the entropy generated during this mixing process can be obtained by assuming the mixing takes place within a short distance downstream of the hole, thus justifying a constant static pressure by using the hole exit



velocity and temperature. This mixing calculation is similar in character to the one-dimensional analytical model proposed by [11].

The mass within the control volume may be expressed mathematically for three dimensional incompressible fluids as:

$$\frac{du}{dx} + \frac{dv}{dy} + \frac{dw}{dz} = 0 \tag{1}$$

The other fundamental equation that governs the flow of a fluid are derived from Newton's second law (the conservation of momentum). The equation is called the Navies-Stokes equation, and for incompressible flow may be expressed in compact Cartesian tensor notation as [12]:

$$\frac{\partial(\rho u_i)}{\partial t} + \frac{\partial(\rho u_j u_i)}{\partial x_j} = -\frac{\partial p}{\partial x_i} + \frac{\partial}{\partial x_i} \left[\left(\frac{\partial u_i}{\partial x_j} + \frac{\partial u_j}{\partial x_i} \right) \right] + S_{bj} \tag{2}$$

where the suffixes i and j represent the co-ordinate directions and (S_{bj}) are buoyancy source or sink terms and are given below:

$$\begin{aligned} S_u &= \frac{\partial}{\partial x} \left(\mu_{eff} \frac{\partial u}{\partial x} \right) + \frac{\partial}{\partial y} \left(\mu_{eff} \frac{\partial v}{\partial x} \right) + \frac{\partial}{\partial z} \left(\mu_{eff} \frac{\partial w}{\partial x} \right) - \frac{\partial p}{\partial x} \\ S_v &= \frac{\partial}{\partial x} \left(\mu_{eff} \frac{\partial u}{\partial y} \right) + \frac{\partial}{\partial y} \left(\mu_{eff} \frac{\partial v}{\partial y} \right) + \frac{\partial}{\partial z} \left(\mu_{eff} \frac{\partial w}{\partial y} \right) - \frac{\partial p}{\partial y} \\ S_w &= \frac{\partial}{\partial x} \left(\mu_{eff} \frac{\partial u}{\partial z} \right) + \frac{\partial}{\partial y} \left(\mu_{eff} \frac{\partial v}{\partial z} \right) + \frac{\partial}{\partial z} \left(\mu_{eff} \frac{\partial w}{\partial z} \right) + \rho g \frac{T_o - T}{T_o} \end{aligned} \tag{3}$$

Energy equation,

$$\begin{aligned} \rho \frac{\partial}{\partial x} (uT) + \rho \frac{\partial}{\partial y} (vT) + \rho \frac{\partial}{\partial z} (wT) &= \frac{\partial}{\partial x} \left(\Gamma_{eff} \frac{\partial T}{\partial x} \right), \\ &+ \frac{\partial}{\partial y} \left(\Gamma_{eff} \frac{\partial T}{\partial y} \right) + \frac{\partial}{\partial z} \left(\Gamma_{eff} \frac{\partial T}{\partial z} \right) + S_T \end{aligned} \tag{4}$$

(μ_{eff}) is the effective viscosity which expressed the combined laminar and turbulent stresses as:

$$\mu_{eff} = \mu + \mu_t \tag{5}$$

(Γ_{eff}) is the effective exchange coefficient for heat defined by:

$$\Gamma_{eff} = \frac{\mu}{\sigma} + \frac{\mu_t}{\sigma_t} \tag{6}$$

The blowing air after leaving the injection hole mixes with main stream. An approximation of the entropy generated during the mixing process can be obtained by assuming that the mixing process takes place within the short



distance downstream of the hole. In the mixing calculation the equations for the conservation of mass and momentum are applied to the mixing control volume.

Flow and heat transfer equations were solved by using the program structure method, which creates the geometry and grid. This method is used in the solver explicitly or implicitly. T-Grid is used to generate a tetrahedron and hexahedron, which are existing boundary mesh.

3 Geometry and flow conditions

Two models, a and b, have been simulated using NACA0021 airfoil for the blade profile, with different compound angles injection from one and two staggered rows arrangement. The holes, dimensions, arrangement and the injection angles used for this study and flow are as follows;

- **Model (a):** The number of holes is (9) on each side, the diameter of hole is $d= 0.1\text{cm}$. Distance between one hole and the other is $5d$, angle of injection $\beta= 37.5^\circ$.

- **Model (b):** Five holes on each side, the diameter of the hole is $d= 0.2\text{ cm}$. Distance between one hole and the other is $5d$, angle of injection $\beta= 90^\circ$.

The schematic diagrams of (NACA 0021) airfoil models and holes arrangement are shown in Figures 1–3.

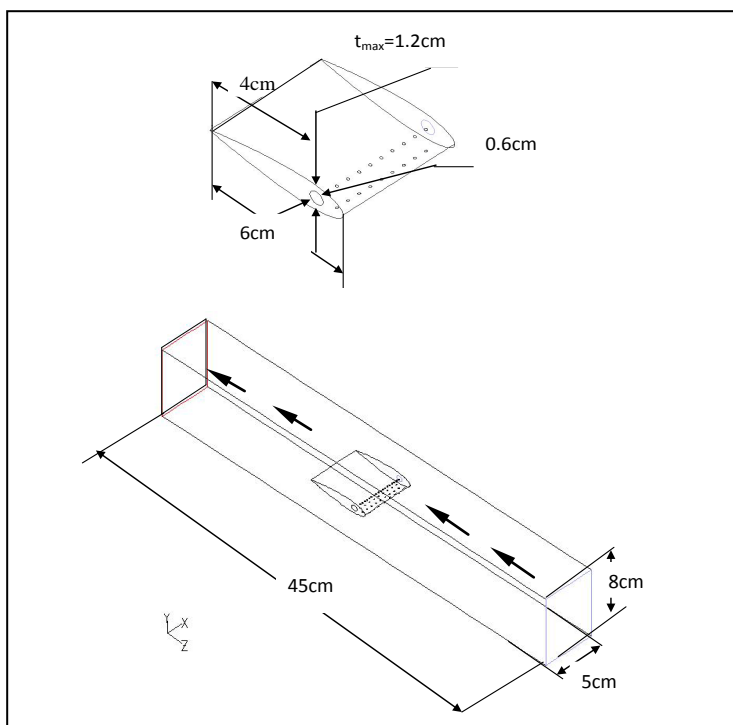


Figure 1: Schematic of test duct.

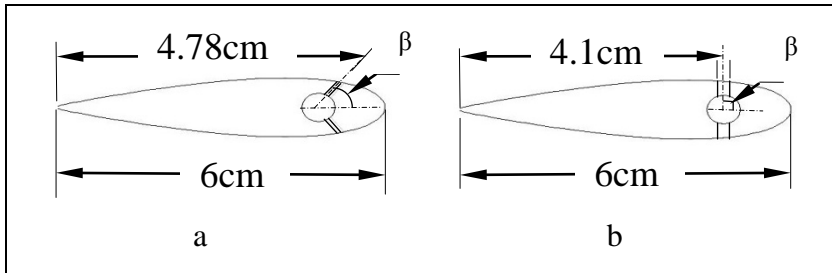


Figure 2: Model a and b (NACA 0021) airfoils.

Grids mesh has kinds such as hexahedron, T-Grid to generate a tetrahedron, which are existing boundary mesh. Program code can use grids comprising of tetrahedron or hexahedron cells, or a combination of the two, in three dimensions. The choice for the problems involved complex geometries; the creation of structured or block-structured grids (consisting of hexahedron cells) can be extremely time-consuming, if not impossible. Set up time is, therefore, the major motivation for using unstructured grids employing tetrahedron cells, the range of length scales of the flow is large, and a tetrahedron mesh can often be created with far fewer cells than the equivalent mesh consisting of hexahedron cells. This is because a tetrahedron mesh allows cells to be clustered in selected regions of the flow domain, whereas structured hexahedron meshes will generally force cells to be placed in regions where they are not needed, the reason behind this case in the current study of unstructured tetrahedron meshes were chosen as shown in Figure 3.

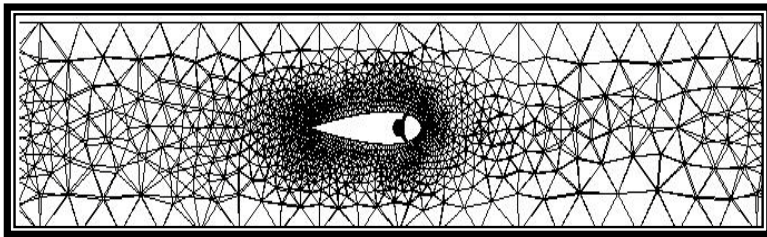


Figure 3: Mesh used in current study in solving Navier-Stokes (K- ϵ standard).

4 Boundary conditions

To define a problem that results a unique solution must be specified. GAMBIT code defining boundary conditions involves information on the dependent (flow) variables at the domain boundaries. Boundary conditions specify the flow and properties variables on the boundaries of the physical model. The boundary conditions in GAMBIT are classified the flow inlet and exit boundaries: free

stream temperature, free stream pressure, jet temperature, model wall surface and the internal face boundary conditions are defined on cell faces, which means that they do not have a finite thickness and they provide a means of introducing a step change in flow properties [14]. The far field boundary conditions are more difficult to specify in a way that facilitates computation.

The boundary conditions in finite volume techniques [15] are used to describe the flow in entry and exit of the solution domain which helps to select the most appropriate boundary condition in application. It provides pressure inlet, jet temperature and velocity, free stream temperature and velocity and wall surface of model [16].

5 Results and discussion

Analysis of computational results is taken at different sections of span-wise direction for the two models. These results are at $x/s=0.5$ and 0.9 .

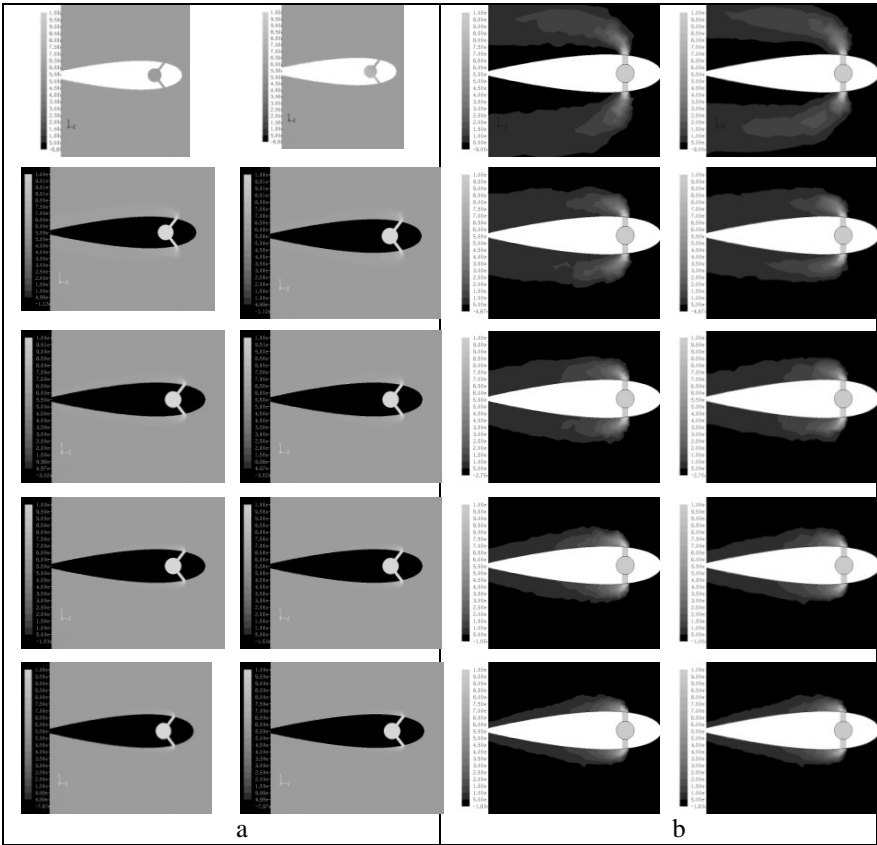


Figure 4: Predictions of adiabatic effectiveness along blade for two models and $\alpha=0^\circ$ with $VR=0.3, 0.7, 1, 1.5, 2$ at $x/s=0.5$ and 0.9 .

Figures 4, 5, and 6 show samples of results of the adiabatic effectiveness contours at $x/s=0.5$ (mid-plane of span and 0.9 for model (a) and (b)). In all cases take into the consideration the injection through which the cooling air issued is at four airfoil angles of attack (0° , 5° , 10° and 15°). The cool jet temperature is (T_j) = 500°K is injected into hot free stream of (T_{in}) = 1300°K for $VR=0.3, 0.5$ and $1.5, 2$.

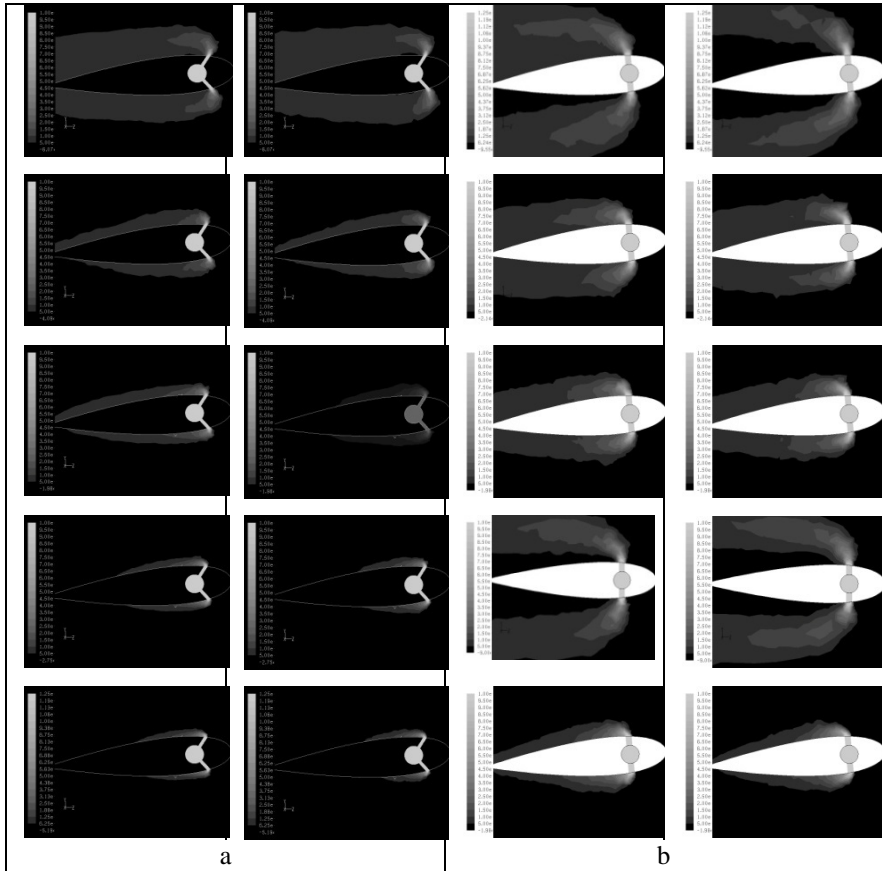


Figure 5: Predictions of adiabatic effectiveness along blade two models *and* $\alpha=5^\circ$ with $VR=0.3, 0.7, 1, 1.5, 2$ at $x/s=0.5$ and 0.9 .

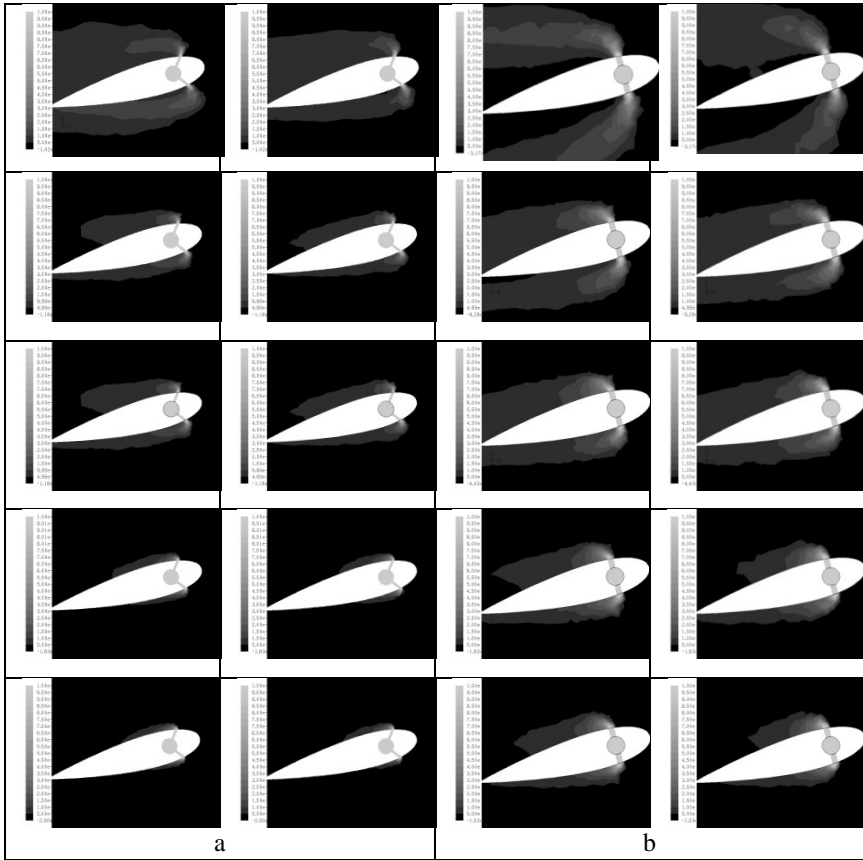


Figure 6: Predictions of adiabatic effectiveness along blade for two models and $\alpha=15^\circ$ with VR=0.3, 0.7, 1.1, 1.5, 2 at $x/s=0.5$ and 0.9 .

The flow is assumed to be a fully developed turbulent flow. A jet lift-off behavior of the contour rotating vortices of the hot free stream under the cool jet can be seen in these figures. In fact, the coolant jet core has actually been divided into two regions at all blowing ratios. In all these figures, high jet penetration in the vertical direction and jet-main stream mixing is observed for ($\alpha= 0^\circ, 5^\circ, 10^\circ$ and 15°), while the penetration area in the stream-wise direction in horizontal plane appears to be weak close to airfoil surface. Thus, the horizontal cooling effect in stream-wise direction close to the surface showed very poor effect for (VR) = 2 angles of attack (10° and 15°).

For the case of VR= 0.9 the two cases of jet angles ($\beta= 37.5^0$) and ($\beta= 90^0$) for angles of attack ($\alpha= 0^0$ and 5^0) gave best cooling effectiveness and high jet penetration. This may be good for the turbine guide vane blade film cooling applications. The blade (airfoil) angle of attack has been varied until optimum film cooling effectiveness, optimum value of the horizontal cooling effect, is obtained. Computational results show jets diameter and issuing angles for maximum film cooling effectiveness (cooling efficiency) agree well with predicted results of [16].

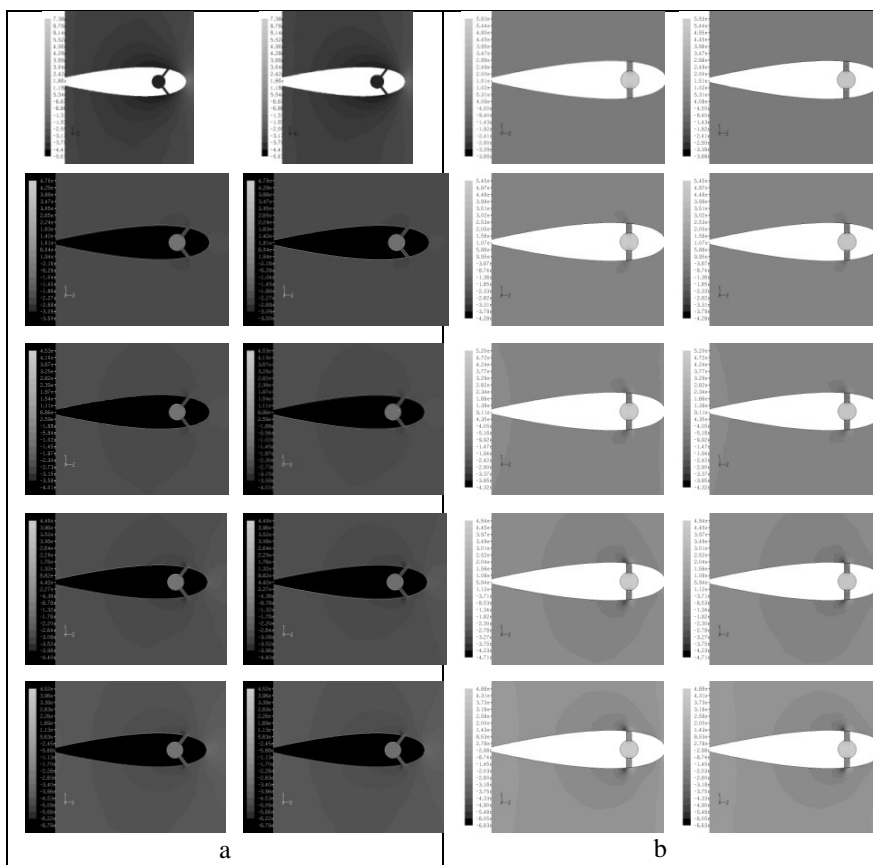


Figure 7: Predictions of pressure coefficients along blade for two models and $\alpha=0$ with VR=0.3, 0.7, 1, 1.5, 2 at $x/s=0.5$ and 0.9.

The results presented in Figures 7, 8 and 9 show samples of results of the pressure coefficient contour at $x/s= 0.5$ (mid-plane of span and 0.9 for model (a) and (b) for VR=0.3, 0.5 and 1.5, 2. Figures showed, as the velocity changes,

so does the dynamic pressure and static pressure according to Bernoulli's principle. Air near the stagnation point has slowed down, and thus the static pressure in this region is higher than the inlet static pressure to main duct. Air that is passing above and below the blade, and thus has speeded up to a value higher than the main inlet path velocity, will produce static pressures that are lower than inlet static pressure. At a point near maximum thickness, maximum velocity and minimum static pressure will occur. Also this figure shows a good agreement with the experimental and computational data of [17].

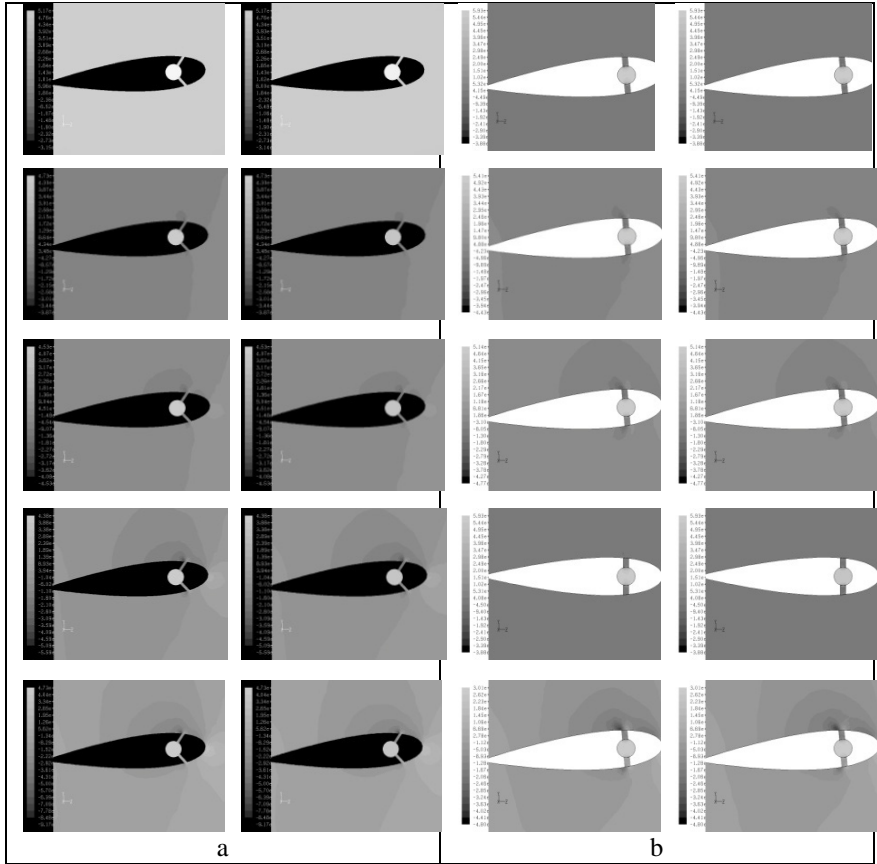


Figure 8: Predictions of pressure coefficients along blade for two models and $\alpha=5^\circ$ with $VR=0.3, 0.7, 1, 1.5, 2$ at $x/s=0.5$ and 0.9 .

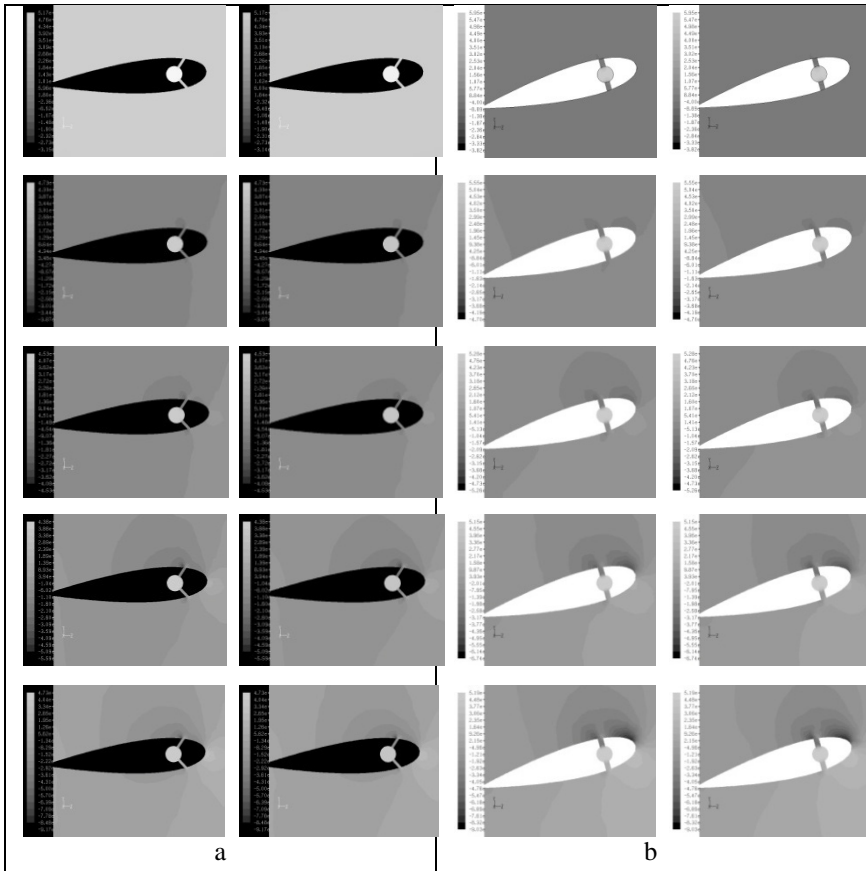


Figure 9: Predictions of pressure coefficients along blade for two models and $\alpha=15^\circ$ with VR=0.3, 0.7, 1, 1.5, 2 at $x/s=0.5$ and 0.9.

6 Conclusions

The analysis of the simulation results revealed that:

- In order to increase the horizontal cooling distance (penetration area in horizontal plane) near the blade surface and to decrease the vertical penetration distance to agreeable distance, there are two methods; either by varying the velocity ratio depending upon jet inclination angles or by decreasing the jets angles.
- The interaction between the neighboring jets enhances the turbulence intensity and diffusion downstream of the jets in the mainstream flow.

Nomenclature

CFD	Computational Fluid Dynamic
C	Chord length (cm)
D	Hole diameter (cm)
i and j	Suffixes represent the co-ordinate direction
NACA	National Advisory Committee of Aeronautics
T	Time-averaged temperature (K)
T _j , T _{in}	Jet temperature and inlet temperature respectively (K)
S _{bj}	Time (sec)
VR	Buoyancy source or sink term
u, v and w	Velocity ratio
x, y and z	Velocity component in x, y and z direction respectively
	Physical or Cartesian Coordinates
α	Blade angle of attack (°)
β	Jet angle with the horizontal axis (°)
ρ	Air density (kg/m ³)
δ	Distance from the wall to the cell center (m)
μ	Dynamic Viscosity (m/N)
τ_w	Wall shear stress N/m ²

References

[1] Ajersch, P., Zhou, J. M., Ketler, S., Salcudean, M. and Gartshore, I. S., “Multiple jets in a cross flow, detailed measurements and numerical simulations”, *ASME Paper 95-GT-9*, 1995.

[2] Theodoridis, G. S., Lakhel, D. and Rodi W., “Three-dimensional calculations of the flow field around a turbine blade with film cooling injection near the leading edge”, *Institute for Hydromechanics, University of Karlsruhe, Kaiserstrasse 12, D-76128, Karlsruhe, Germany*, 2001.

[3] Bunker, R., “Film Cooling Effectiveness Due to Discrete Holes Within a transverse Surface Slot,” *ASME Paper GT-2002-30178*, 2002.

[4] Waye, S., and Bogard, D., “High-Resolution Film Cooling Effectiveness Measurements of Axial Holes Embedded in a Transverse Trench With Various Trench Configurations”, *Journal of Turbomachinery*, 129, 294, DOI: 10.1115/1.2464141, 2007.

[5] Rallabandi, A.P., Grizzle, J., and Han, J.C., “Effect of upstream step on flat plate film cooling effectiveness using PSP”, 2008 Proceedings of the ASME Summer Heat Transfer Conference, HT08-56194, vol. 2, 599–609, Jacksonville, FL, United States, 2008.

[6] Gao, Z., and Han, J.C., “Influence of Film-Hole Shape and Angle on Showerhead Film Cooling Using PSP Technique”, *Journal of Heat Transfer*, 131(6), 061701 (pages 11), DOI:10.1115/1.3082413, 2009.



- [7] Je-Chin Han and Akhilesh P. Rallabandi, "Turbine Blade Film Cooling Using PSP Technique", *Frontiers in Heat and Mass Transfer*, 1, 013001 DOI: 10.5098/hmt.v1.1.3001, 2010.
- [8] Kini, Chandrakant R, Shenoy B, S., Sharma, N Yagnesh, "A Computational Conjugate Thermal Analysis of HP Stage Turbine Blade Cooling with Innovative Cooling Passage Geometries", *Proceedings of the World Congress on Engineering Vol III, London, U.K., 2011.*
- [9] Azzi, A., Abidat, M., Jubran, B. A. and Theodoridis G.S., 2001, "Film cooling predictions of simple and compound angle injection from one and two staggered rows", *Numerical Heat Transfer, Part A, Vol. 40*, pp. 237–294, 2001.
- [10] Hussein, M. A., "Experimental and computational simulation of turbine blade film cooling flow; Effect of jet angle", *PHD Thesis, University of Technology, Al-Rasheed College of Engineering and Science, Baghdad, Iraq, June 2006.*
- [11] Lene, K. H. and Bjorn, H. H., "CFD modeling of turbulent mixing in a confined wake flow", *Aalborg University, Esbjerg, 2003.*
- [12] Vestige, H. K. and Malalasekera, W., "An introduction to computational fluid dynamics", finite volume method, *Longman Group, London, 1996.*
- [13] Yang, Z. and Shih, T. H., "New time scale based k- ϵ model for near – wall turbulence", *AIAA, J 31 (7)*, pp. 1191–1197, 1993.
- [14] FLUENT, 6.1, code, fluent users.com, 2002.
- [15] Leylek, J. H. and Zerkle, R. D., "Discrete-jet film cooling", *ASME paper 93-GT-207*, 1993.
- [16] Karcz, M., "Performance analysis of the thermal diffusers, the gas turbine cooling aspects", *PhD Thesis, Institute of fluid-flow machinery PAS, Thermo-chemical power department, Gdansk, Poland, 2003.*
- [17] Yousif, H., Al-Khishali, K.M., and Kassim, Muna S., "Investigation of leading edge film cooling jets on cross flow", *Journal of Engineering and Development*, 2 (15), pp. 103–119, 2011.

